Polymer Vol. 39 Nos. 6–7, pp. 1475–1481, 1998

0032-3861/97/$17.00+0.00

PII: S0032-3861(97)00417-5

Characterization of curdlan in aqueous sodium hydroxide

Mitsuo Nakata[a],*, Tsuyoshi Kawaguchi[a], Yuzo Kodama[a] and Akira Konno[b]
[a]*Department of Polymer Science, Faculty of Science, Hokkaido University, Sapporo, 060, Japan*
[b]*Kinran College, Suita, 565, Japan*
(Received 20 September 1996; revised 21 March 1997)

Curdlan ((1 → 3)-β-D-glucan) was found to be fractionated through liquid–liquid phase equilibrium with the mixture dimethyl sulfoxide + lithium chloride as a solvent and acetone as a precipitant. Light scattering and viscosity measurements were made on solutions of fractionated samples in 0.3 M NaOH in the range of the molecular weight M_w from 5.3×10^4 to 2.0×10^6. The observed intrinsic viscosity $[\eta]$ was analysed by the Yamakawa–Fujii–Yoshizaki theory of a wormlike chain, and the persistence length, molecular weight per unit contour length and molecular diameter were determined roughly as 6.8 nm, 890 g nm^{-1} and 1.1 nm, respectively. These molecular parameters represented the molecular weight dependence of $[\eta]$ and the mean-square radius of gyration $\langle s^2 \rangle_z$, reasonably indicating an effect of the excluded volume at large M_w. Detailed behaviour of curdlan in 0.3 M NaOH could not be revealed on account of a large uncertainty caused by microgel aggregates in the light scattering measurements. © 1997 Elsevier Science Ltd. All rights reserved.

(Keywords: curdlan; (1 → 3)-ß-D-glucan; static light scattering)

INTRODUCTION

Curdlan is a bacterial polysaccharide composed entirely of (1 → 3)-ß-D-glucosidic linkage and differs only in the linkage manner of repeating units from cellulose [1–4]. This polysaccharide is highly crystalline [5,6] and exhibits various gelation mechanisms depending on the chain conformation [7–10]. In addition curdlan has been studied from the view point of antitumour activity [11–13]. These characteristics of curdlan may be caused by the specific chain conformation due to (1 → 3)-ß-D-glucosidic linkage.

As for dilute solution properties of curdlan, a few studies have been made with alkali solutions [14] and with cadoxen, known as a solvent for cellulose [15]. Experiments made on an unfractionated sample in sodium hydroxide solution suggested a conformational transition from helical structure to random coil with increasing alkali concentration from 0.19 to 0.24 M. A similar conformational transition was also observed in lithium hydroxide solution [14]. Curdlan was found to be fractionated with cadoxen as a solvent and propanol + water mixture as a precipitant. The molecular weight dependence of the mean-square radius of gyration and intrinsic viscosity observed for fractionated samples indicated that the conformation of curdlan is partly of random coil in the solvent of 1:1 water-diluted cadoxen [15].

Difficulty in fractionation of curdlan has hampered studies of the dilute solution which requires samples of narrow molecular weight distribution and of various molecular weights. Therefore, it is desirable to find out a convenient solvent + precipitant system for the fractionation of curdlan; cadoxen [16] is not familiar in usual laboratories. On account of the high crystallinity, curdlan tends to precipitate in a form of fibre or to cause gelation in solvent + precipitant systems without yielding liquid–liquid phase separation. For this reason alkali solutions could not be employed as a solvent for fractionation.

In this paper curdlan was found to be soluble in the mixture dimethyl sulfoxide (DMSO) + lithium chloride (LiCl). The curdlan solution in this mixture exhibited liquid–liquid phase equilibrium with clear interface, when acetone was added as a precipitant. Thus, curdlan could be fractionated in this solvent + precipitant system by the precipitational method. We made light scattering and viscosity measurements for the fractionated samples in sodium hydroxide solution and obtained preliminary data of molecular weight dependence of the intrinsic viscosity $[\eta]$, mean-square radius of gyration $\langle s^2 \rangle$ and second virial coefficient A_2. As for the chain conformation and gelation mechanism, curdlan exhibits an interesting behaviour in sodium hydroxide solution, while in this solvent there exist microgel aggregates which cause considerable difficulty in light scattering measurements.

EXPERIMENTAL

Materials

The original sample of curdlan was supplied in the form of spray-dried powder from Takeda Chemical Industries Ltd., Osaka, Japan. To obtain purified samples with various molecular weight, fractionation was carried out for both sonicated and unsonicated curdlan. The mixture DMSO + LiCl at 0.05 g ml^{-1} in LiCl concentration was used as a solvent. The fractionated samples were designated as listed in *Table 1*. The series CUD3 of lower molecular weight was prepared as follows. Curdlan weighing 15 g was dissolved in 900 ml of the solvent DMSO + LiCl and sonicated at

---

* To whom correspondence should be addressed

Table 1 Light scattering and viscosity data obtained for fractionated samples of curdlan

Sample	$10^{-6}M_w$	$10^{11}\langle s^2\rangle$ (cm^2)	10^4A_2 (mol cm^3 g^{-2})	$[\eta]$ (cm^{3}g^{-1})
CUD1-F2	2.02	6.39	4.2	665
CUD1-F3	1.91	6.70	4.1	643
CUD1-F4	1.81	5.54	3.6	590
CUD1-F5	1.45	4.64	4.5	520
CUD1-F6	1.28	3.99	5.0	468
CUD1-F7	1.26	3.33	3.6	443
CUD1-F8	1.12	3.41	3.6	387
CUD1-F9	0.95	2.56	3.9	343
CUD1-F10	0.91	2.58	2.7	295
CUD3-F2	0.56	1.85	6.1	238
CUD3-F3	0.50	1.62	6.0	218
CUD3-F4	0.45	1.18	5.6	200
CUD3-F5	0.39	1.16	6.4	165
CUD3-F6	0.28	0.74	6.1	140
CUD3-F7	0.23	0.57	5.4	129
CUD3-F8	0.17	0.36	7.4	96
CUD3-F9	0.092	0.29	6.0	60
CUD4-F2	0.053	0.11	10.9	38

18°C for 24 h with the usual ultrasonic cleaner. The effect of the sonication was evaluated by measuring the flow time of the solution of a constant volume through a capillary tube. When the flow time decreased from the initial time 1730 s to 170 s by sonication, acetone of 980 ml was added to the solution and it was stirred vigorously at 20°C. Further addition of 10 ml of acetone brought about sudden cloudiness. By raising the temperature, the solution became transparent near 27°C and again cloudy near 50°C, indicating upper and lower cloud point temperatures. The solution was kept at 17°C overnight and liquid–liquid phase equilibrium was formed with a clear interface between two transparent phases. The upper phase was transferred into another flask for further fractionation. The lower phase, rich in curdlan, was diluted moderately by the solvent DMSO + LiCl and precipitated into the mixture acetone + water (1:1 by volume) of a large volume to collect curdlan. The precipitate was washed several times in the acetone + water mixture and finally in acetone for vacuum drying. This fraction was labelled as CUD3-F1. From the upper phase transferred into the other flask the second fraction, CUD3-F2, was obtained as in the case of CUD3-F1.

The series CUD1 of higher molecular weight was obtained from unsonicated curdlan. The procedure of the fractionation of this series is essentially the same as that of the series CUD3. Curdlan weighing 7 g was dissolved in 1400 ml of the solvent. Acetone was added to the solution to bring about the cloud point, which appeared abruptly at the volume 1571 ml of added acetone. The solution did not recover transparency by being warmed. By keeping the clouded solution at a constant temperature overnight, it became transparent, forming liquid–liquid phase equilibrium with a clear interface. The further procedure of the fractionation was the same as in the case of CUD3. Thus, we obtained 11 and 10 fractions for the series CUD1 and CUD3, respectively.

CUD4-F2 was fractionated from well-sonicated curdlan to obtain a low molecular weight sample. CUD5-F5 was fractionated from unsonicated curdlan with care to remove low molecular weight components.

Solution preparation

Since curdlan is known to undergo degradation in alkaline solution [14], the preparation of curdlan solutions and subsequent measurements were carried out without time interruption. The curdlan sample was put in NaOH aqueous solution and stirred for 150 min to make a stock solution. To prepare solutions at lower concentrations the stock solution was diluted by the NaOH aqueous solution and stirred for 30 min.

Fractionated samples did not dissolve in NaOH aqueous solution at low concentrations less than 0.15 M or so, while the original sample in the form of spray-dried powder dissolved in NaOH aqueous solutions as low as 0.01 M. Solutions of fractionated samples at low NaOH concentrations were prepared by diluting curdlan solutions at 0.3 M NaOH with pure water.

Viscosity measurements

Viscosity measurements were performed at 25°C with the Ubbelohde-type viscometer just after the solution preparation. To determine the intrinsic viscosity $[\eta]$ at each NaOH concentration, the measurements were made at four curdlan concentrations. $[\eta]$ was estimated from the intercept of the plots of η_{sp}/c *versus* c and $\ln \eta_r/c$ *versus* c, where c is the curdlan concentration, and η_{sp} and η_r are the specific and relative viscosities, respectively. These plots yielded straight lines with a common intercept. Since the viscometer had moderately high shear rate as 800 s^{-1} for the present solvent, the shear-rate dependence of $[\eta]$ was estimated with a three-bulb viscometer. For the sample of the highest molecular weight the effect of the shear rate was found to be 5%, which was not so significant compared with the uncertainty in the present light scattering experiment.

Refractive index increment measurements

Refractive index increments $(\partial n/\partial c)_{u_2}$ at constant composition of solvent and $(\partial n/\partial c)_{\mu}$ at constant chemical potentials of all solvent components were determined at 25°C with a differential refractometer of the Brice type [17]. Here, the subscript u_2 denotes the volume fraction of NaOH in the solvent for pure components. It should be remembered that the quantities for NaOH are signified by the subscript 2 and those for curdlan have no subscript as the concentration c. Refractive index increments were measured for the sample CUD5-F5 with the molecular weight $M_w = 1.25 \times 10^6$ at wavelengths of 436 nm and 633 nm. Dialysis of curdlan solutions was made with a 10 ml stainless steel cell, which was immersed in 300 ml of solvent contained in a plastic bottle. The solution in the cell, which was essentially the same with an osmometer, was stirred by a Teflon-coated magnetic rod to accelerate attainment of dialysis equilibrium. A couple of days were required for the dialysis equilibrium. The refractive index increment at 0.3 M NaOH was obtained as $(\partial n/\partial c)_{u_2} = 0.143$ at 436 nm, 0.138 at 633 nm, and $(\partial n/\partial c)_\mu = 0.160$ at 436 nm and 0.155 at 633 nm. Measurements of the refractive index increment were also made at 0.1, 0.22 and 0.3 M NaOH with the original sample. $(\partial n/\partial c)_{u_2}$ was determined to be 0.143 at 436 nm and 0.139 at 633 nm, irrespective of NaOH concentration. However, $(\partial n/\partial c)_\mu$ at 0.3 M NaOH was underestimated as 0.144 at 436 nm and 0.140 at 633 nm, which indicated diffusible components in the original curdlan.

The differential refractometer could be also used to determine the variation in the refractive index of the solvent with NaOH concentration. In the concentration range from 0.1 M to 0.4 M, we obtained the constant values $dn/dw_2 = 0.283$ at 436 nm and 0.271 at 633 nm at 25°C, where w_2 is the weight fraction of NaOH in the solvent.

Light-scattering measurements

The measurements were carried out at 25°C with unpolarized incident light at 435.8 nm [17]. The photometer was calibrated with benzene as standard and operated at intervals of 15° in the angular range from 30° to 135°.

For optical clarification each solution was filtered through Sartorius membrane filter (SM250) into a solution cell of 22-mm i.d. and again filtered into the same cell. The solution cell was immersed in a cylindrical cell filled with the mixture of methanol + water, which had the refractive index matched with that of the solution. The scattered intensities were measured at 30 min after the set-up of the cylindrical cell in the photometer.

It should be noted that in the optical clarification the filtration of the solutions of the original sample could be made smoothly with a filter of 0.2-μm pore size. However, the filtration was not easy for solutions of fractionated samples, though we used a filter of 0.2 or 0.45-μm pore size, depending on curdlan concentration and molecular weight. The high resistance in the filtration may be ascribed to microgel aggregates because of the high crystallinity of curdlan. Light scattering data obtained for filtered solutions did not show strong forward scattering characteristic to large particles. However, for lower molecular weight samples, the angular dependence of scattered intensities appeared to be affected by the forced filtration. Thus, the mean-square radius of gyration $\langle s^2 \rangle$ of low molecular weight samples could not be determined reliably.

Light scattering data analysis

Scattered intensities at an angle of θ were transformed into the excess Rayleigh's ratio R_θ and analysed by the equation [18]

$$(Kc/R_\theta)^{1/a} = (1/M^{1/a})\{1 + (1/3a)\langle s^2 \rangle q^2 + (2/a)MA_2C\} \quad (1)$$

with

$$K = (2\pi^2 n^2 / N_A \lambda^4)(\partial n/\partial c)_\mu^2$$

$$q = (4\pi n/\lambda)\sin(\theta/2)$$

where N_A is Avogadro's number, λ is the wavelength of incident light in a vacuum, and n is the refractive index of solution. The use of $(\partial n/\partial c)_\mu$ reflects the fact that the curdlan solution may be a ternary system of a polymer in a mixed solvent [19].

In equation (1) the scattering function $P(x)$ with $x = \langle s^2 \rangle q^2$ is assumed to be written as

$$P(x) = (1 + x/3a)^{-a} \quad (2)$$

which may be compared with the Debye scattering function for a random flight polymer chain [20]

$$P(x) = (2/x^2)(e^{-x} - 1 + x) \quad (3)$$

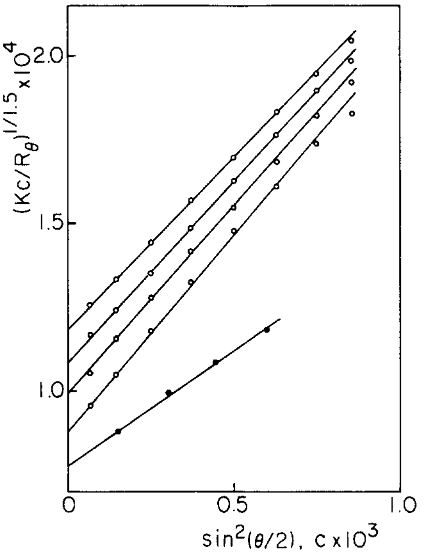

Figure 1 Light scattering data for CUD1-F5 in 0.3 M NaOH by plots of $(K_c/R_\theta)^{1/1.5}$ *versus* $\sin^2(\theta/2)$ (○) and $(K_c/R_0)^{1/1.5}$ *versus* c (•)

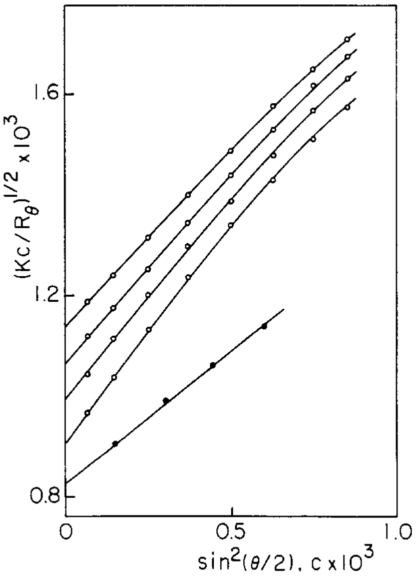

Figure 2 Light scattering data for CUD1-F5 in 0.3 M NaOH by plots of $(K_c/R_\theta)^{1/2}$ *versus* $\sin^2(\theta/2)$ and $(K_c/R_0)^{1/2}$ *versus* c as in *Figure 1*

For $a = 1.5$ equation (2) approximates equation (3) numerically within an error of 1.4% in the range $x < 8.6$. Accordingly, the plot of $(Kc/R_\theta)^{1/1.5}$ *versus* $\sin^2 \theta/2$ for experimental data becomes practically linear in a broad range of x yielding $< s^2 >$ reliably [18]. Berry has proposed the root plot with $a = 2$ in view of the wide range for the initial slope [21].

In *Figures 1 and 2* the light scattering data obtained for the sample CUD1-F5 are given by the plot of $(Kc/R_\theta)^{1/a}$ *versus* $\sin^2 (\theta/2)$ with $a = 1.5$ and 2, respectively. $(Kc/R_0)^{1/a}$ extrapolated to $\theta = 0$ is plotted against the concentration c with the filled circles. In the plot with $a = 1.5$ the data points at each c are represented by a straight line, slope of which increases slightly with decreasing c. For the root plot with $a = 2$, the data points at each c are described by a curved line and the initial slope increases with decreasing c. For each plot $\langle s^2 \rangle_z$ was evaluated from the value of the slope extrapolated to $c = 0$, and M_w and A_2 were estimated from the intercept and slope of the plot of $(Kc/R_0)^{1/a}$ *versus* c according to equation (1). It should be noticed that the plot of $(Kc/R_\theta)^{1/1.5}$ *versus* $\sin^2 \theta/2$ gives M_w and $\langle s^2 \rangle_z$ without resorting to data points at low angles, which may be affected more or less by microgel aggregates. Thus, we analysed the present light scattering data by the plot with $a = 1.5$. The obtained values of M_w, $\langle s^2 \rangle_z$ and A_2 are listed in *Table 1*.

Analysis of $[\eta]$ *and* $\langle s^2 \rangle$

Figure 3 shows a plot of $[\eta]$ *versus* NaOH concentration observed for the sample CUD3-F4 at 25°C. In the range from 1.6 M to 2.5 M, $[\eta]$ changes rapidly with a sharp depression near 0.22 M. The curdlan chain has been reported to have a helical conformation at low NaOH and a coil conformation at high NaOH with a transition region near 0.22 M NaOH [7,14]. Thus, the sharp depression at 0.22 M NaOH in *Figure 3* may be attributed to the conformational transition of curdlan chain. This characteristic behaviour of $[\eta]$ invokes a helix–coil transition observed for poly-L-glutamic acid [22], though the polypeptide has a low degree of polymerization near 280 and the value of $[\eta]$ is about one-fifth of the present one. Since in the present study $\langle s^2 \rangle_z$, A_2 and $[\eta]$ were determined as a function of M_w at 0.3 M NaOH, we first tried to analyse the data with the solution theory of flexible polymer chain.

In *Figures 4–6* the logarithm of $[\eta]$, $\langle s^2 \rangle_z$ and A_2 is plotted against M_w, respectively. In *Figure 6* the straight line depicted as a guide for the data points gives $A_2 = 0.028\, M_w^{-0.3}$, which may be compared with that for a polymer in a good solvent in magnitude and molecular weight dependence. In *Figure 4* the data points were found to fall on a straight line which was represented by $[\eta] = 0.0079\, M_w^a \,\mathrm{cm^3\, g^{-1}}$ with $a = 0.78$. In *Figure 5* the data points were roughly described by a straight line given by $\langle s^2 \rangle_z^{1/2} = 0.036\, M_w^{\nu}$ nm with $\nu = 0.53$. The exponent $a = 0.78$ may be comparable with that for a polymer in a good solvent, while $\nu = 0.53$ is typical of a polymer in a poor solvent. To reveal the relation between $[\eta]$ and $\langle s^2 \rangle_z$, we evaluated the Flory viscosity constant Φ ($= [\eta]M/(6\langle s^2 \rangle)^{3/2}$). The above molecular weight dependences of $[\eta]$ and $\langle s^2 \rangle_z$ yield $\Phi = 1.2 \times 10^{22} M_w^{0.19}$, which increases from 0.9×10^{23} to 1.9×10^{23} with increasing M_w in the experimental range of M_w and is much smaller than the usual value near 2.5×10^{23}. It is obvious that the data of the curdlan solution are not explained by the conventional two-parameter theory of flexible polymer chains [23].

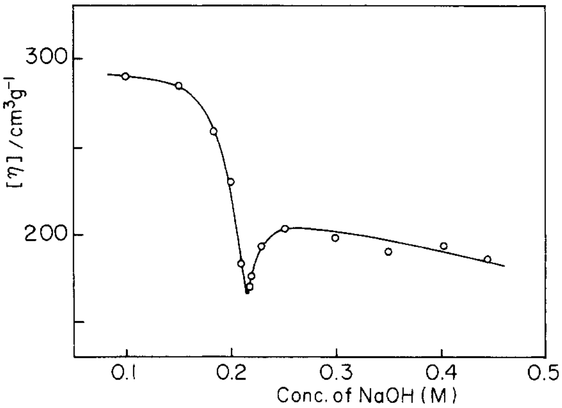

Figure 3 $[\eta]$ as a function of NaOH concentration for sample CUD3-F4 at 25°C

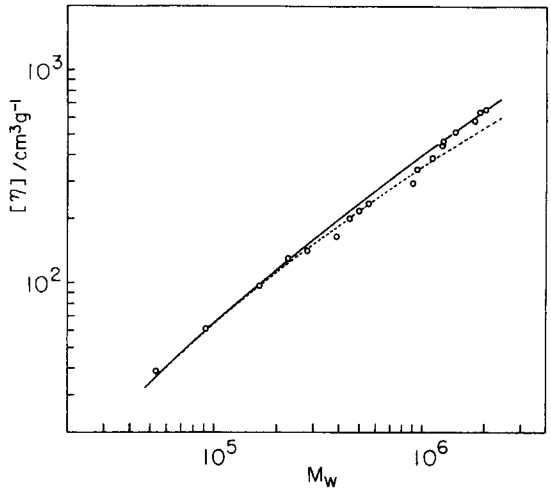

Figure 4 Log–log plot of $[\eta]$ *versus* M_w for curdlan in 0.3 M NaOH at 25°C. Solid and dotted lines correspond to Yamakawa–Fujii–Yoshizaki theory with $2q = 13.5$ nm, $M_L = 890\ \mathrm{g\ nm^{-1}}$ and $d = 1.10$ nm. For the solid line, the excluded-volume effect is taken into account by equation (10) and equation (13)

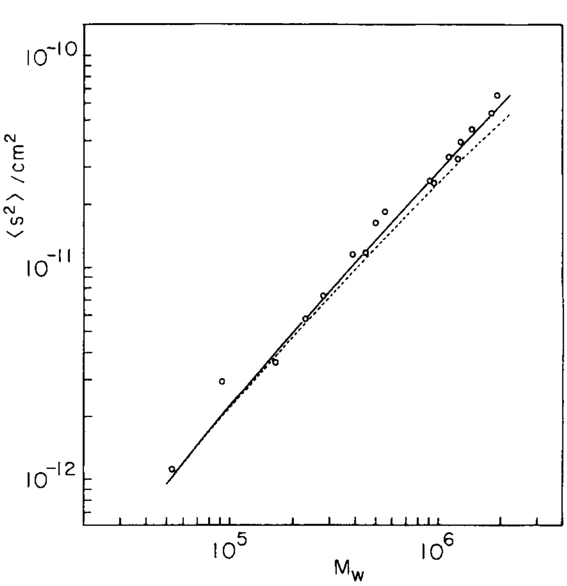

Figure 5 Log–log plot of $\langle s^2 \rangle_z$ *versus* M_w for curdlan in 0.3 M NaOH at 25°C. Solid and dotted lines are due to equation (9) with the same molecular parameters as in *Figure 4*. For the solid line, the excluded-volume effect is taken into account by equation (10) and equation (14)

For stiff-chain polymers the intrinsic viscosity $[\eta]_0$ at an unperturbed state has been derived numerically on the basis of a continuous wormlike chain model with the molecular parameters of the chain contour length L, the persistence length q and the molecular diameter d [24,25]. L is related to the molecular weight M by $L = M/M_L$, where M_L is the molecular weight per unit contour length of the chain. The persistence length q is related to the Kuhn statistical segment length λ^{-1} by $2q = \lambda^{-1}$ and the relation $(\langle R^2\rangle_0/M)_\infty = 2q/M_L$ holds at the limit of the random-flight chain ($L \to \infty$), where $\langle R^2\rangle_0$ is the unperturbed mean-square end-to-end distance. In view of a practical use for data analysis, the numerical expressions for $[\eta]_0$ (cm^3 g^{-1}) were approximated by an analytical equation as [26]

$$(M^2/[\eta]_0)^{1/3} = I + SM^{1/2} \qquad (4)$$

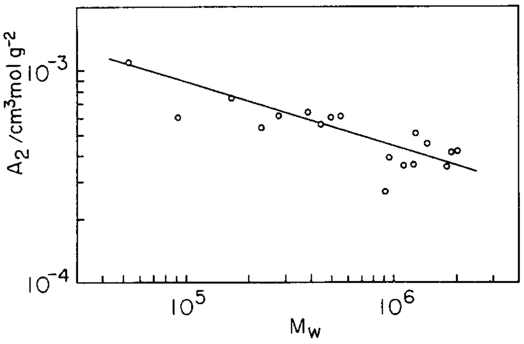

Figure 6 Log–log plot of A_2 *versus* M_w for curdlan in 0.3 M NaOH at 25°C. The solid line is described by eye

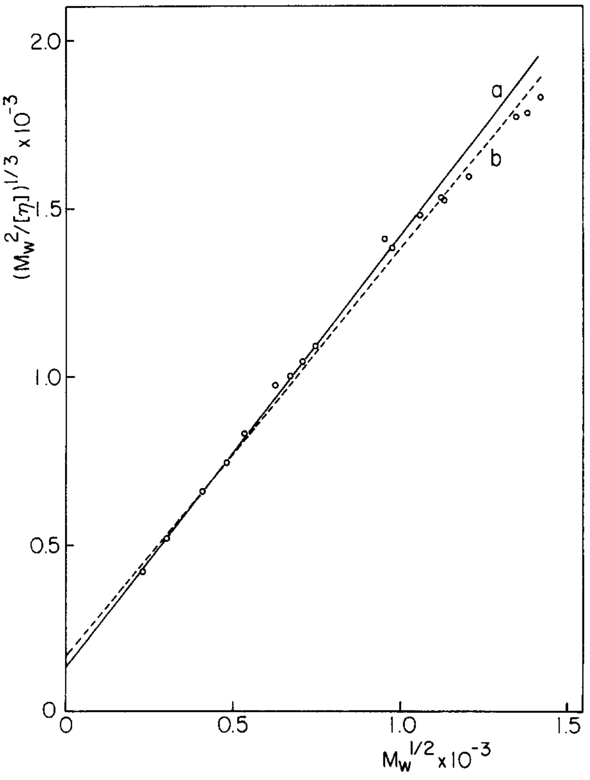

Figure 7 Plot of $(M^2/[\eta])^{1/3}$ *versus* $M^{1/2}$ according to equation (4). The solid line a is fitted to data points at small $M^{1/2}$. The broken line b is fitted to data points with some weight at large $M^{1/2}$

where

$$I = 1.52 \times 10^{-8} I_0 M_L \qquad (5)$$

and

$$S = 1.52 \times 10^{-8} S_0 (2q/M_L)^{-1/2} \qquad (6)$$

Here, I_0 and S_0 are given as functions of $d/2q$. According to equation (4), I and S can be evaluated from the intercept and slope of the plot $(M^2/[\eta]_0)^{1/3}$ *versus* $M^{1/2}$, respectively. To determine the three molecular parameters another relation is necessary in addition to equations (5) and (6). It may be reasonable to employ the relation for the partial specific volume $\bar{v}$ of the polymer molecule given by

$$\bar{v} = (\pi N_A/4)(d^2/M_L) \qquad (7)$$

Since S_0 decreases slowly from 1.11 to 1.00 with increasing $d/2q$ from 10^{-3} to 1.0, S_0 may be approximated by the average value 1.05. Thus, equations (5)–(7) yield

$$(d/2q)^2/I_0 = 0.497(\bar{v}S^4/I) \qquad (8)$$

Since $\log[(d/2q)^2/I_0]$ is given as a linear function of $\log(d/2q)$ explicitly, $d/2q$ can be easily estimated from the value of $\bar{v}S^4/I$.

Figure 7 shows the plot due to equation (4) for the present data. The solid line a is fitted to the data points at smaller $M^{1/2}$. The downward curvature at higher $M^{1/2}$ might stem from the excluded volume effect. However, this deviation cannot be taken seriously because of an experimental uncertainty. The broken line b is fitted to the data points with some weight at larger $M^{1/2}$. $\bar{v}$ was assumed to be a reciprocal of the density 1.50 g cm^{-3} calculated from X-ray data for hydrated curdlan[6]. We obtained $I = 140$ and $S = 1.28$ from the line a and $I = 170$ and $S = 1.21$ from the line b. For both the cases, equation (8) and the relations of $\log[(d/2q)^2/I_0]$ and S_0 to $\log(d/2q)$ yielded $S_0 = 1.04$, which did not agree with the average value $S_0 = 1.05$. Thus, we determined the molecular parameters with $S_0 = 1.04$. The results are $2q = 13.5$ nm, $M_L = 890$ g nm^{-1} and $d = 1.10$ nm for the line a, and $2q = 17.5$ nm, $M_L = 1030$ g nm^{-1} and $d = 1.17$ nm for the line b. The dotted lines in *Figures 4 and 5* are described with the molecular parameters due to the line a. For the calculation of $\langle s^2\rangle_z$, we used the relation [27]

$$\langle s^2\rangle_0 = (qL/3)\{1 - 3(q/L) + 6(q/L)^2 - 6(q/L)^3 \times [1 - \exp(-L/q)]\} \qquad (9)$$

In *Figures 4 and 5* the dotted lines deviate downward from the data points at large $M^{1/2}$, suggesting the excluded-volume effect. The molecular parameters due to the line b in *Figure 7* yielded lines of better fit to the data points with smaller downward deviation at large $M^{1/2}$ in *Figures 4 and 5*. We introduced the excluded-volume effect by $\langle s^2\rangle = \langle s^2\rangle_0 \alpha_s^2$ and $[\eta] = [\eta]_0\alpha_\eta^3$, α_s and α_η being expansion factors.

In the wormlike chain model the expansion factors are given as a function of the scaled excluded volume parameter $\tilde{z}$ defined by [28–30]

$$\tilde{z} = (3/4)K(\lambda L)z \qquad (10)$$

with

$$z = (3/2\pi)^{3/2}(\lambda B)(\lambda L)^{1/2} \qquad (11)$$

$$K(L) = 4/3 - 2.711L^{-1/2} + (7/6)L^{-1} \qquad (12)$$

Here, z is the conventional excluded-volume parameter, B is a parameter proportional to the binary cluster integral, and the function $K(L)$ is valid for $L > 6$. According to recent data analyses [31,32] of $[\eta]$ and $\langle s^2 \rangle$ we used the equations of the expansion factors given by [33,34]

$$\alpha_\eta^3 = (1 + 3.8\tilde{z} + 1.9\tilde{z}^2)^{0.3} \tag{13}$$

and

$$\alpha_s^2 = [1 + 10\tilde{z} + (70\pi/9 + 10/3)\tilde{z}^2 + 8\pi^{3/2}\tilde{z}^3]^{2/15} \times [0.933 + 0.067\exp(-0.85\tilde{z} - 1.39\tilde{z}^2)] \tag{14}$$

The solid lines in *Figures 4 and 5* are given with the aid of equation (13) and equation (14), respectively, with the molecular parameters for line a and $\lambda B = 0.05$, which was determined to make an agreement with the data points. The molecular parameters due to line b and $\lambda B = 0.02$ yielded lines close to the respective solid lines in *Figures 4 and 5*.

We tried to calculate the characteristic ratio C_∞ according to

$$C_\infty = \lim_{n \to \infty} (6\langle s^2 \rangle_0 / nb^2) \tag{15}$$

where n is the number of the monomer unit and b is the bond length. For the glucopyranose as a monomer unit, we used the molecular weight 162 and the virtual bond length [35] $b = 0.485$ nm and obtained $C_\infty = 10.5$ and 11.7 from $\langle R^2 \rangle_0 / M = 0.0152\ \mathrm{nm}^2$ and $0.0170\ \mathrm{nm}^2$, respectively.

The molecular parameters obtained from lines a and b in *Figure 7* are not very different from each other and the difference may be taken as a measure for the experimental uncertainty. Since the two sets of the molecular parameters could describe the experimental data equally well, we use the parameters due to line a in the following discussion.

DISCUSSION

The obtained value $C_\infty = 10.5$ is appreciably larger than theoretical values for (1 → 3)-ß-D-glucan [35,36]. Since this value is comparable with those for synthetic polymers such as polystyrene (~10.0) [37], curdlan in 0.3 M NaOH solution may be relatively flexible. This seems to explain the fact that the light scattering data for CUD1-F5 with $M_w = 1.45 \times 10^6$ are represented reasonably by the Debye scattering function in *Figures 1 and 2*. This molecular weight gives the number of Kuhn segments as $L/(2q) = 121$, and in equation (9) $\langle s^2 \rangle_0$ can be approximated by the leading term $qL/3$ with an error of 1%. For the sample CUD3-F9 with $M_w = 9.2 \times 10^4$, however, $L/(2q)$ remains to be only 8 and $\langle s^2 \rangle_0$ is smaller 21% than $qL/3$.

Curdlan has been known as to form triple helix in crystalline state [5,6]. X-ray diffraction data for hydrated curdlan yield $M_L = 520\ \mathrm{g\ nm^{-1}}$ for a single chain, which is roughly half the present value of $890\ \mathrm{g\ nm^{-1}}$. It is interesting to determine M_L in the helix region at low NaOH concentration. The triple helical structure in the crystalline state was found to be maintained for schizophyllum in aqueous solutions [38,39]. For the original sample and CUD3-F4 light scattering measurements were made at 0.01 M NaOH and 0.1 M NaOH, respectively. The obtained molecular weights agreed with the corresponding molecular weights determined at 0.3 M NaOH.

A few studies of single chain conformation of (1 → 3)-ß-D-glucan have been made so far. Hirano *et al.* carried out light scattering and viscosity measurements on fractionated samples of curdlan in the 1:1 water-diluted cadoxen [15]. Since cadoxen, which was used as a solvent for the fractionation, could dissolve curdlan molecularly, the light scattering measurements appear to be made reliably without being disturbed by microgel aggregates. The experimental results were summarized as $\langle s^2 \rangle_z^{1/2} = 3.2 \times 10^{-2} M_w^{0.53}$ nm for $M_w > 0.7 \times 10^5$ and $[\eta] = 2.5 \times 10^{-4} M_w^{0.65}\ \mathrm{cm^3\ g^{-1}}$ for $M_w > 2 \times 10^5$. Thus, the curdlan chain in the water-diluted cadoxen is appreciably contracted compared with that in the 0.3 M NaOH solution. Schizophyllum dissolves in dimethylsulfoxide as a single chain [39]. The single chain was considered to be flexible from the viscosity exponent $a = 0.69$. By the way, curdlan chain in 0.3 M NaOH has a contracted conformation compared with cellulose chain observed in different solvents [16,40,41].

The preferential sorption coefficient λ is practically defined by the equation [42]

$$(\partial n/\partial c)_\mu = (\partial n/\partial c)_{u_2} - \lambda(\partial n/\partial u_2)_c \tag{16}$$

where u_2 is the volume fraction on the basis of pure substance. For dilute polymer solutions $(\partial n/\partial u_2)_c$ can be replaced by dn/du_2 for solvent. From the data of dn/dw_2 we obtained $dn/du_2 = 0.601$ at 436 nm and 0.577 at 633 nm with $2.13\ \mathrm{g\ ml^{-1}}$ for the density of pure NaOH. Then, λ was calculated as − 0.029 irrespective of wavelength. The negative λ means extra ions of NaOH in coil domain. According to a thermodynamic argument λ can be written as [42]

$$\lambda = -\{V_2(1 - u_2)/M\}(\partial m_2/\partial m)_\mu \tag{17}$$

where m_2 and m are the molalities of NaOH and curdlan in solution, respectively, and V_2 is the molar volume of pure NaOH. $(\partial m_2/\partial m)_\mu$ provides a rough measure of the number of molecules added or removed from the coil domain of a polymer [43]. The values of $V_2 = 18.8\ \mathrm{ml\ g^{-1}}$, $M = 1.25 \times 10^6$ and $u_2 = 0.0056$ give $(\partial m_2/\partial m)_\mu = 1900$, which corresponds to an extra 0.25 NaOH molecules per repeating unit in the coil domain. Here, the volume of a coil domain was assumed to be given by $(4\pi/3)\langle s^2 \rangle^{3/2}$.

The curdlan samples used in this study seems to have a narrow molecular weight distribution on account of the fractionation. From the weights and molecular weights of the samples of the series CUD1, the weight- and number-average molecular weights of the original sample were estimated to be $M_w = 1.44 \times 10^6$ and $M_n = 1.17 \times 10^6$, respectively. These values yield the molecular weight distribution $M_w/M_n = 1.23$ for the original sample. On the other hand, we obtained $M_w/M_n = 1.61$ for the sonicated curdlan from the data of the samples of the series CUD3. The molecular weight distribution of the original sample is very narrow compared with those of synthetic polymers prepared by radical polymerization. By sonication the molecular weight distribution became wider to some extent. In both the series CUD1 and CUD3 the molecular weight of the fraction decreases with increasing fraction number. In the light of the narrow molecular weight distribution of the original curdlan, this successive separation of curdlan indicates a high efficiency of the fractionation and, consequently, the samples of the series CUD3 as well as CUD1 are expected to have a narrow molecular weight distribution. However, the first fractions were coloured unsuitably for measurement and the last fractions were discarded because of the unexpectedly low intrinsic viscosity.

The calculated molecular weight $M_w = 1.44 \times 10^6$ for the original sample was considerably larger than $M_w = 1.07 \times 10^6$ obtained directly by light scattering measurement. This difference might be attributed to very low molecular weight components which could not be collected as a sample in the fractionation process. This conjecture is compatible with the smaller value of $(\partial n/\partial c)_\mu$ obtained for the original sample than for the sample CUD5-F5 as mentioned in the Experimental section.

ACKNOWLEDGEMENTS

We thank Vitamin & Food Company, Takeda Chemical Industries Ltd, for supplying the curdlan sample.

REFERENCES

1. Maeda, I., Saito, H., Masada, M., Misaki, A. and Harada, T., *Agric. Biol. Chem.*, 1967, **31**, 1184.
2. Harada, T., Misaki, A. and Saito, H., *Arch. Biochem. Biophys.*, 1968, **124**, 292.
3. Saito, H., Misaki, A. and Harada, T., *Agric. Biol. Chem.*, 1968, **32**, 1261.
4. Nakanishi, I., Kimura, K., Kusui, S. and Yamazaki, E., *Carbohydr. Res.*, 1974, **32**, 47.
5. Deslandes, Y., Marchessault, R. H. and Sarko, A., *Macromolecules*, 1980, **13**, 1466.
6. Chuah, C. T., Sarko, A., Deslandes, Y. and Marchessault, R. H., *Macromolecules*, 1983, **16**, 1375.
7. Saito, H., Ohki, T. and Sasaki, T., *Biochem.*, 1977, **16**, 908.
8. Harada, T., *ACS Symp. Ser.*, 1977, **45**, 265.
9. Saito, H., Tabeta, R., Sasaki, T. and Yoshioka, Y., *Bull. Chem. Soc. Jpn*, 1986, **59**, 2093.
10. Saito, H., Yosioka, Y., Yokoi, M. and Yamada, J., *Biopolymers*, 1990, **29**, 1689.
11. Sasaki, T. and Takasuka, N., *Carbohydr. Res.*, 1976, **47**, 99.
12. Sasaki, T., Abiko, N., Sugano, Y. and Nitta, K., *Cancer Res.*, 1978, **38**, 379.
13. Yoshioka, Y., Tabeta, R., Saito, H., Uehara, N. and Fukuoka, F., *Carbohydr. Res.*, 1985, **140**, 93.
14. Ogawa, K., Watanabe, T., Tsurugi, J. and Ono, S., *Carbohydr. Res.*, 1972, **23**, 399.
15. Hirano, I., Einaga, Y. and Fujita, H., *Polym. J.*, 1979, **11**, 901.
16. Henley, D., *Arkiv. Kemi.*, 1961, **18**, 327.
17. Nakata, M., Kawate, K. and Ishitaka, Y., *Macromolecules*, 1994, **27**, 1825.
18. Nakata, M., *Polymer*, 1997, **38**, 9.
19. Takashima, K., Nakae, K., Shibata, M. and Yamakawa, H., *Macromolecules*, 1974, **5**, 641.
20. Debye, P., *J. Phys. Colloid Chem.*, 1947, **51**, 18.
21. Berry, G. C., *J. Chem. Phys.*, 1966, **44**, 4550.
22. Doty, P., Wada, A., Yang, J. T. and Blout, E. R., *J. Polym. Sci.*, 1957, **23**, 851.
23. Yamakawa, H., *Modern Theory of Polymer Solutions*. Harper & Row, New York, 1971.
24. Yamakawa, H. and Fujii, M., *Macromolecules*, 1974, **7**, 128.
25. Yamakawa, H. and Yoshizaki, T., *Macromolecules*, 1980, **13**, 633.
26. Bohdanecky, M., *Macromolecules*, 1983, **16**, 1483.
27. Benoit, H. and Doty, P., *J. Phys. Chem.*, 1953, **57**, 958.
28. Yamakawa, H. and Stockmayer, W. H., *J. Chem. Phys.*, 1972, **57**, 2843.
29. Yamakawa, H. and Shimada, J., *J. Chem. Phys.*, 1985, **83**, 2607.
30. Shimada, J. and Yamakawa, H., *J. Chem. Phys.*, 1986, **85**, 591.
31. Abe, F., Einaga, Y. and Yamakawa, H., *Macromolecules*, 1993, **26**, 1891.
32. Hayashi, K., Tsutsumi, K., Nakajima, F., Norisuye, T. and Teramoto, A., *Macromolecules*, 1995, **28**, 3824.
33. Domb, C. and Barrett, A., *Polymer*, 1976, **17**, 179.
34. Barrett, A., *Macromolecules*, 1984, **17**, 1566.
35. Cleland, R. L., *Biopolymers*, 1971, **10**, 1925.
36. Whittington, S. G. and Glover, R. M., *Macromolecules*, 1972, **5**, 55.
37. Flory, P. J., *Statistical Mechanics of Chain Molecules*. Interscience, New York, 1969.
38. Yanaki, T., Norisuye, T. and Fujita, H., *Macromolecules*, 1980, **13**, 1462.
39. Kashiwagi, Y., Norisuye, T. and Fujita, H., *Macromolecules*, 1981, **14**, 1220.
40. Valtasaari, L., *Makromol. Chem.*, 1971, **150**, 117.
41. McCormick, C. L., Callais, P. A. and Hutchinson, B. H., *Macromolecules*, 1985, **18**, 2394.
42. Chu, S. G. and Munk, P., *Macromolecules*, 1978, **11**, 879.
43. Dondos, A. and Benoit, H., *Macromolecules*, 1973, **6**, 242.